Effect of Isocyanates on the Crystallinity and Thermal Stability of Polyurethanes

Y. M. SONG,[1] W. C. CHEN,[1] T. L. YU,[1,*] K. LINLIU,[2,†] and Y. H. TSENG[3]

[1]Department of Chemical Engineering, Yuan Ze Institute of Technology, Nei-Li, Taoyuan, Taiwan 32026, [2]Department of Chemical Engineering, National Tsing Hua University, Hsinchu, Taiwan 30043, and [3]Chemical Fiber Plant, Far Eastern Textile Co. Ltd., Hsinpu, Hsinchu, Taiwan 30509

SYNOPSIS

Polyurethanes were synthesized from polyester and butanediol with three different diisocyanates, i.e., 4,4'-diphenylmethane diisocyanate (MDI), *m*-xylene diisocyanate (XDI), and 2,4-toluene diisocyanate (TDI). The effect of chemical structures of diisocyanate compounds on the degree of crystallinity and the thermal stability were observed. Differential scanning calorimetry (DSC) and small-angle X-ray scattering (SAXS) were used to determine the degree of crystallinity of the hard segment. The thermal degradation of polyurethanes was studied by the thermogravimetric method. It has been shown that the polyurethane hard-segment crystallinity decreases in the following order: MDI > XDI > TDI. The experimental results also indicated that polyurethanes with aralkyl diisocyanates, i.e., XDI, had the best thermal stability. The polyurethanes synthesized from aromatic diisocyanates, i.e., MDI and TDI, had worse thermal stability than from XDI. However, owing to the higher degree of hard-segment crystallinity for polyurethanes from MDI, these polyurethanes had a better thermal stability than those based on TDI. © 1996 John Wiley & Sons, Inc.

INTRODUCTION

Properties of segmented polyurethanes depend on the structure of hard and soft segments, their length, and concentration, as well as the interaction of both phases. Usually the soft segment is based on polytetramethylene oxide or aliphatic polyester and the hard segment on butanediol (BD) and diisocyanate compounds such as diphenylmethane diisocyanate (MDI), xylene diisocyanate (XDI), and toluene diisocyanate (TDI). Being of different chemical nature from the soft segments, the hard segment tend to separate in the matrix due to immiscibility of both phases and tend to associate into "domains" forming physical crosslinks.[1-6] While hard segment is glassy or semicrystalline at room temperature, the soft segment phase is in the rubbery state. Polyesters synthesized from adipic acid and low molecular weight glycols are crystalline homopolymers having melting points around 50°C. However, polyester soft segments in polyurethanes lose the ability to crystallize for short segment length, due to steric hindrances. Because crystallization of the soft segments is an undesirable property, it can be avoided by copolymerization or, as in some commercial prepolymers, by inserting TDI or other irregularities into the soft segments.

Generally speaking, polyurethanes are thermally very stable polymers. The onset degradation temperature of the urethane bond depends on the type of isocyanate and glycol used. It is a general rule that the more easily formed urethanes are less stable, i.e., more easily dissociated than are the more difficult ones. Thus, the highest degradation temperature, above 250°C, is observed for a urethane formed from alkyl isocyanate and alkyl alcohol, followed by aryl isocyanate–alkyl alcohol, alkyl isocyanate–aryl alcohol, and an aryl isocyanate–aryl alcohol combinations.[7,8]

In this work, crystallinity and thermal stability of segmented polyurethanes based on aliphatic polyester and three diisocyanates, i.e., MDI, XDI,

* To whom correspondence should be addressed.
† Present address: Vanguard International Semiconductor Corp., Science-Based Industrial Park, Hsinchu, Taiwan 30077.

Journal of Applied Polymer Science, Vol. 62, 827–834 (1996)
 CCC 0021-8995/96/050827-08

and TDI, with butanediol as chain extender were studied by differential scanning calorimetry (DSC), small-angle X-ray scattering (SAXS), and thermogravimetric analysis (TGA).

EXPERIMENTAL

Materials

Polyester–Diol

Aliphatic polyester was synthesized from adipic acid (Riedel–de Haen Co.), hexanediol (Riedel–de Haen Co.), and 1,2-propanediol (Riel–de Haen Co.) by condensation polymerization under nitrogen atmosphere. The mole ratio of adipic acid/hexanediol/1,2-propanediol was 1.0/0.73/0.46. The final polymer had an acid value of 3 mg KOH/g, and the molecular weight M_n determined by GPC (Waters model 746 GPC with μ-styrogel columns of pore sizes 500 Å, 10^3 Å and 10^4 Å, and a RI detector) was found to be 1750 with a dispersion of M_w/M_n = 1.80 at 25°C. Tetrahydrofuran (THF) was used as the mobile phase, and narrow MWD polystyrene standards (Aldrich Chemical Co.) were used in the linear calibration of chromatographic measurement.

Polyurethane

Three polyurethanes were synthesized from polyester-diol and diisocyanate compound, i.e., MDI (Tokyo Kasei Kogyo Co.), XDI (Riedel–de Haen Co.), and 2,4-TDI (Tokyo Kasei Kogyo Co.), with butanediol as chain extender by prepolymerization method. Polyester–diol was first reacted with diisocyanate at 90–100°C for 1 h under nitrogen atmosphere. The prepolymer was then cooled down to room temperature and reacted with butanediol under N_2 atmosphere for 20 min. Table I shows the mole ratios of polyester–diol/diisocyanate/butanediol of three polyurethanes (i.e., PU-M, PU-X, PU-T) synthesized in our lab. Before polymerization polyester–diol and butanediol were distilled at 70°C under vacuum for 1 h to remove moisture. All of the final polyurethanes had a soft segment content of approximately 51.8 wt %. Polyurethane films were compression molded at 200°C for 10 min on a press (Tien Fa Co, Taiwan, ROC) followed by cooling at ambient temperature.

Differential Scanning Calorimetry (DSC)

A Du Pont 910 DSC was used to study the soft segment glass transition and the endotherms of hard segment crystalline structure. Hermetic DSC pans were used for the measurements with calibration by Indium pellet. The weight of the sample was around 8–10 mg. All of the experiments were carried out with a heating rate of 10°C/min.

Small-angle X-ray Scattering (SAXS)

Small-angle X-ray scattering measurements were performed with a Rigaku Denki slit collimated X-ray cameras, the radiation source of which is an 18 kW rotating anode generator with Cu target, to be operated at 100 mA and 40 keV (installed at the Department of Nuclear Engineering, National Tsing Hua University, Taiwan). The smearing effect of SAXS was compensated by a pinhole, graphite collimator to monochromatize the incident x-ray beams on the sample. The scattered intensity was detected by a two-dimension photodiode array detector (Oak Ridge Detector Laboratory, Inc.) with 256 × 256 Channels (1 mm between each pixel). The sample to detector distance is 400 cm in length. All data were corrected for background (dark current) and the sensitivity of each pixel in the area detector. For amorphous system, the area of scattered pattern was radially averaged to increase the efficiency of data collection comparison with one-dimension linear detector. The experimental scattering $I(q)$ data at $q \to 0$ and $q \to \infty$ are usually noisy and need correction. In this experiment, the low q end data were corrected according to Debye–Bueche theory,[9] while the high q end data according to Porod–Ruland theory.[10,11]

Table I Chemical Composition of Polyurethanes

Samples	Molar Ratio			Soft Segment Content (wt %)
	Polyester–Diol	Diisocyanate	Butanediol	
PU-M	0.410	2.10	1.590	51.8
PU-X	0.335	2.10	1.665	51.8
PU-T	0.317	2.11	1.683	51.8

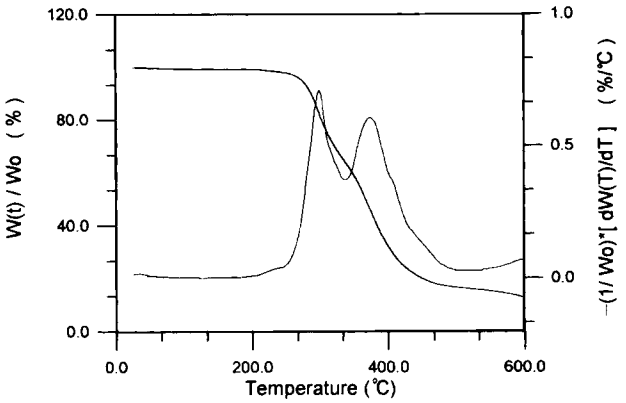

Figure 1 Plots of TGA and DTGA curves for PU-M sample.

Thermogravimetric Analysis (TGA)

The kinetics of degradation of segmented polyurethanes was measured using about 10 mg sample in DuPont 1090 Thermal Analyzer with TGA model 910. Heating rates of 2°C/min, 5°C/min, and 10°C/min were used under a nitrogen flow rate kept 50 mL/min.

RESULTS AND DISCUSSION

TGA Analysis

The TGA weight loss curve displays two distinct regions of weight loss that are reflected in the differential weight loss (DTGA) curve. Figure 1 is the plots of TGA and DTGA curves for the PU-M sample. Several researchers have studied the thermodegradation of polyurethanes by TGA, and established that the amount of weight loss of the first region was well correlated with the hard segment concentration, suggesting that the degradation started in the hard segment.[7,12] As shown in Figure 1, the first part of the degradation correlates with the hard segment, while the second peak correlates with the degradation of the soft segment. Qualitative characterization of the degradation process is illustrated by the onset and maximum peak temperatures of the first step, T_{1on} and T_{1max}, along with the same for the second step, T_{2on} and T_{2max}. Table II summarizes T_{1on}, T_{1max}, T_{2on}, and T_{2max} of samples PU-M, PU-X, and PU-T.

The degradation process can be characterized by activation energy, measured with TGA experimental data using three analytical methods. Because the mechanism changes during the degradation of polyurethanes, activation energy is not only a function of chemical structure of polymers but also varies with the conversion. It provides a parameter for the assessment of the thermal stability of polyurethanes.

The first method of calculating the activation energy was proposed by Flynn.[13,14] This method is applied to low conversions, between 1 and 5 % of nonisothermal differential weight loss (DTGA) method with a constant heating rate β. The conversion, α, is defined by[13,14]

$$\alpha = 1 - w(t)/w_o \tag{1}$$

where w_o and $w(t)$ represent initial weight and weight at any time, t, during degradation, respectively. According to Flynn et al.,

$$\frac{d}{d\alpha}\left[T^2 \frac{d\alpha}{dT}\right] = \frac{E_a}{R} + 2T \qquad (\alpha < 0.05 \quad \text{and} \quad \beta = \text{constant}) \tag{2}$$

where T is the Kelvin temperature, E_a the activation energy, and R the gas constant. Figure 2 is the plots of $(T^2 d\alpha/dT)$ vs. α for three polyurethane samples (i.e., PU-M, PU-X, and PU-T). The activation energies calculated from eq. (2) for these samples are summarized in Table III.

The second method of calculating activation energy, proposed by Ozawa and Flynn,[15,16] requires several TGA curves at different heating rates (β). It consists of plotting the logarithm of heating rate ($\log \beta$) versus $1/T$ for each degree of conversion (α). From these isoconversion curves, activation energy

Table II TGA Parameters of Polyurethanes

Samples	$T_{1\,on}$ (°C)	$T_{1\,max}$ (°C)	$T_{2\,on}$ (°C)	$T_{2\,max}$ (°C)
PU-M	245.0	299.6 (0.189)	337.3 (0.401)	371.4 (0.621)
PU-X	250.0	320.0 (0.235)	333.5 (0.339)	386.7 (0.736)
PU-T	242.0	296.9 (0.308)	323.5 (0.470)	371.9 (0.737)

The numeric values in parentheses are the conversions, α, at the corresponding temperatures.

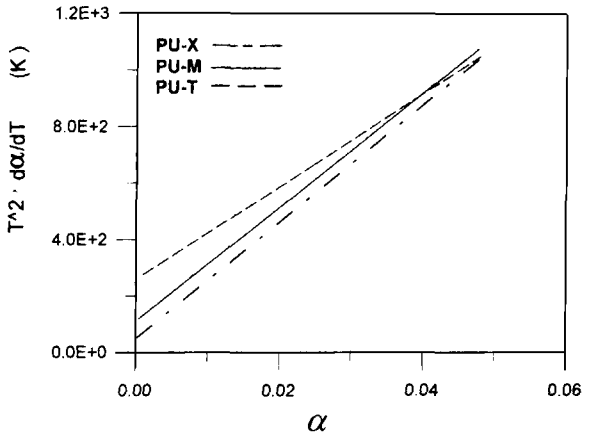

Figure 2 Plots of eq. (2) for PU-M, PU-T, and PU-X.

was calculated from the slope of the lines using the expression

$$E_a = -(\text{slope})R/0.457 \tag{3}$$

where R is the gas constant. Figure 3 is the plots of $\log \beta$ versus $1/T$ for PU-T sample at four conversions (i.e., $\alpha = 0.1$, $\alpha = 0.3$, $\alpha = 0.5$, and $\alpha = 0.7$). Similar results were also obtained for PU-M and PU-X. Table IV lists the activation energies for these three polyurethanes calculated by the Ozawa–Flynn method.

The third method need only one nonisothermal TGA measurement.[17-19] The decomposition rate can be expressed by an equation[20]:

$$d\alpha/dt = k(1 - \alpha)^n \tag{4}$$

where α is defined by eq. (1), $d\alpha/dt$ is the decomposition rate, n is the empirical order of decomposition, and k is the decomposition rate constant that can be expressed by the Arrhenius equation:

$$k = A \exp(-E_a/RT) \tag{5}$$

where A is the frequency factor (1/min). Substituting eq. (5) into eq. (4), which can be rewritten in the form

$$d\alpha/dt = A \exp(-E_a/RT)(1 - \alpha)^n \tag{6}$$

Experiments in thermal analysis were carried out at a constant heating rate, β (K/min) = dT/dt. Equation (6) can be rewritten as

$$d\alpha/dT = (A/\beta)\exp(-E_a/RT)(1 - \alpha)^n \tag{7}$$

Table III TGA Activation Energy of Hard Segment [Eqs. (2) and (8)]

Samples	Flynn [Eq. (2)] (J/mol)	Eq. 8 (J/mol)
PU-M	1.59×10^5	1.26×10^5
PU-X	1.64×10^5	1.39×10^5
PU-T	1.36×10^5	9.15×10^4

Equation (7) can also be transformed to the following form:

$$\ln\left[\frac{d\alpha/dT}{(1 - \alpha)^n}\right] = -\frac{E_a}{RT} + \ln(A/\beta) \tag{8}$$

A plot of $\ln[(d\alpha/dT)/(1 - \alpha)^n]$ against $1/T$ will yield a straight line to fit the data in which the decomposition order n can be selected. The slope of the line will provide the activation energy and the intercept for the frequency factor. Chang[17] fitted the experimental data of polyurethane elastomers to the simulated curves and found that the decomposition order was very close to $n = 1$. The plots of $(d\alpha/dT)/(1 - \alpha)^n$ versus $1/T$ at a heating rate $\beta = 5$°C/min with the decomposition order $n = 1$ for PU-M, PU-X, and PU-T are shown in Figure 4. The activation energies of decomposing hard segment were calculated from the slope of the curves at the temperature ranges $T_{1on} \sim T_{1max}$ for samples of PU-M, PU-X, and PU-T and are summarized in Table III.

Comparing the T_{1on}, T_{1max}, and E_a of these three polyurethanes, it is obvious that the thermal stability of the hard segments of these polyurethanes are in following order PU-X > PU-M > PU-T. It is well known that aliphatic diisocyanates impart better light and thermal stability to polyurethanes derived

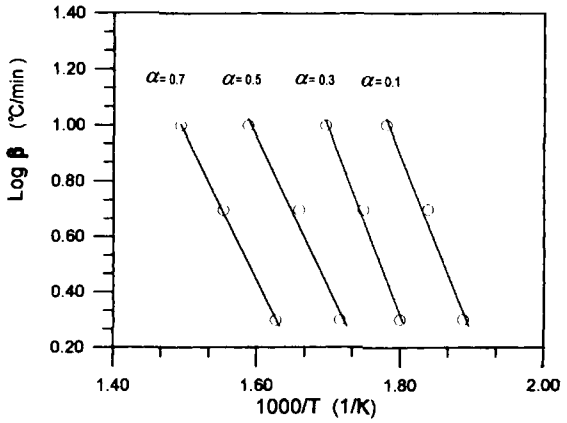

Figure 3 Plots of $\log \beta$ vs. $1/T$ for PU-T at four conversions ($\alpha = 0.1$, $\alpha = 0.3$, $\alpha = 0.5$, and $\alpha = 0.7$).

from them than from aromatic diisocyanates.[21-23] Thus, the present finding of better thermal stability of PU-X than that of PU-M and PU-T is consistent with the results reported in literatures.

The weight percent and chemical structure of the soft segments of these three polyurethanes were same. However, the values of T_{2on} and conversion α corresponding to T_{2on} for these three polyurethanes were quite different (Table II). The values of T_{2on} and its corresponding conversion α of PU-T were lower than those of PU-M and PU-X. The results of DSC and SAXS analyses, as shown in the following sections, revealed that these three polyurethanes have the following order of hard segment crystallinity: PU-M > PU-X > PU-T. It is obvious that the thermal stability and degree of crystallinity of hard segment have a great influence on the thermal stability of soft segment. The higher thermal stability and higher degree of crystallinity of hard segment leaded to a higher degradation temperature of soft segment (T_{2on}).

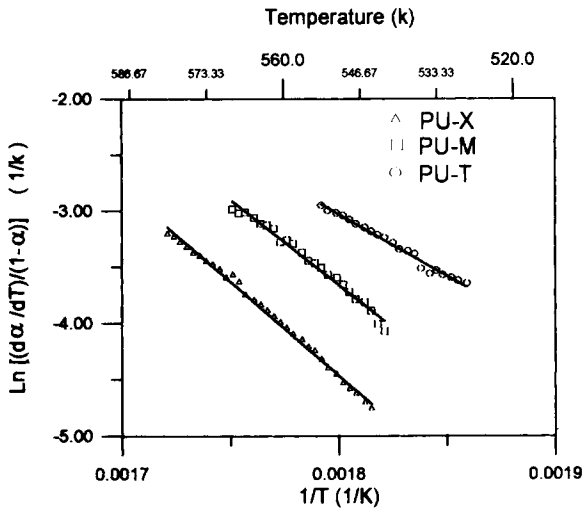

Figure 4 Plots of eq. (8) for the hard segments of PU-M, PU-T, and PU-X.

DSC Analysis

Differential scanning calorimetric (DSC) method is a well-established method to study the morphology of segmented polyurethanes.[24,25] The nonisothermal DSC scanning curves provide the information of glass transition of the amorphous soft segment, endortherm of the crystallized soft segment, and the endortherm of the crystallized hard segment. Figure 5 is the plots of nonisothermal DSC scanning curves (with a heating rate of 10°C/min) for PU-M, PU-T, and PU-X. The transition around −20 to −40°C corresponds to the glass transition temperature (T_g) of polyester soft segment, while the endortherm between 150–200°C corresponds to the melting temperature (T_m) of hard segment.[24,25] Table V lists T_g of the polyester soft segment, T_m of hard segment, and heat of fusion (ΔH) of the hard segment for these three polyurethanes. The results of the lowest soft segment T_g, highest hard segment T_m, and highest ΔH of heat of fusion of the hard segment for PU-M revealed a better phase separation between the soft and hard segments and the highest degree of hard segment crystallinity in these three polyurethanes. From Figure 5 and Table V, we also know that PU-T has a higher soft segment T_g than PU-M and PU-X, and no hard segment endortherm was observed for PU-T. These results indicated the phenomenon of phase mixing between hard and soft segments, and a lowest degree of crystallinity of the hard segment was observed for PU-T. In summary of these DSC data, we may draw the following order of degree of hard segment crystallinity: PU-M > PU-X > PU-T.

SAXS Analysis

The structural morphology of segmented polyurethane was investigated using a rotating angle SAXS. The microphase separation transition in block copolymers as well as their structure parameters such as interdomain spacing (L), core zone thickness (d_0), and transition zone thickness (d_{tr}) (interface thickness) of partially crystalline polymers were analyzed by a one-dimensional correlation function that is the Fourier transformation

Table IV Activation Energies of Polyurethanes (Ozawa–Flynn Method)

Samples	α = 0.1 (J/mol)	α = 0.3 (J/mol)	α = 0.5 (J/mol)	α = 0.7 (J/mol)
PU-M	1.33×10^5	1.44×10^5	1.46×10^5	1.64×10^5
PU-X	1.64×10^5	1.78×10^5	1.85×10^5	1.37×10^5
PU-T	1.17×10^5	1.22×10^5	9.85×10^4	9.57×10^4

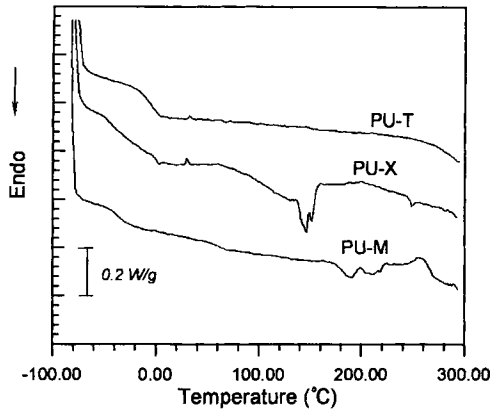

Figure 5 Plots of nonisothermal DSC scanning curves (heating rate 10°C/min) for PU-M, PU-T, and PU-X.

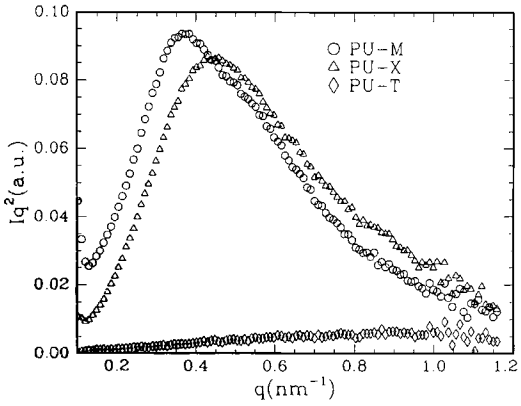

Figure 6 Lorentz corrected SAXS curves for PU-M, PU-X, and PU-T.

of scattering intensity function based on the model of Strobl and Schneider.[26]

In this work, two-dimensional small-angle x-ray scattering (SAXS) patterns of PU-M, PU-X, and PU-T were obtained. For the lamellar structure of block copolymers, the scattered intensity function should be treated with Lorenz correction by multiplying $I(q)$ with q^2, i.e., $I(q)q^2$.[27,28] The Lorentz corrected SAXS curves for PU-M, PU-X, and PU-T are shown in Figure 6; here **q** is the scattering vector, $q = [4\pi \sin(\theta/2)]/\lambda$, with λ being the wave length of incident X-ray, and θ the scattering angle, respectively). The invariant quantity Q of overall mean square electron density fluctuation is obtained by integrating $q^2I(q)$ all over the scattering angle.

$$Q = \frac{1}{2\pi^2}\int_0^\infty q^2 I(q)dq \tag{9}$$

The value of invariant Q describes the electron density fluctuation of polymer and is a good approximation to estimate the overall degree of phase separation in segmented polyurethane. The interdomain spacing, L, can be estimated from the q_m corresponding to the maximum of $I(q)q^2$ versus q curves (Fig. 6) using the Bragg equation:

$$L = 2\pi/q_m \tag{10}$$

Table VI summarizes the Q values and the L values estimated from eqs. (9) and (10), respectively, of three different polyurethanes, i.e., PU-M, PU-X, and PU-T, among which PU-M and PU-X have larger values of Q than PU-T, due to the electron dendity contrast between MDI- and XDI-based hard segment, and the soft segment is larger than that of TDI-based polyurethanes. The other reason for a lower Q value of PU-T may be due to the less degree of phase separation between soft and hard segments (as shown in the nonisothermal DSC scans).

Structural parameters such as inter domain spacing (L), interfacial thickness (d_{tr}), core zone (d_0), and lamellar thickness (d) can also be determined from 1-D correlation function $\gamma_1(r)$ obtained from the Fourier transformation of scattering intensity curve. The normalized 1-D electron density correlation function, $\gamma_1(r)$, can be expressed by[26]

$$\gamma_1(r) = \frac{1}{Q}\int_0^\infty q^2 I(q)\cos(qr)dq \tag{11}$$

The method for the determination of L, d_{tr}, d_0, and d is shown in Figure 7. On the left hand side of Figure 7, it shows the electron density distribution

Table V DSC Data of Polyurethanes

Samples	T_g (°C) of Soft Segment	T_m (°C) of Hard Segment	ΔH (J/g)
PU-M	−37.3	178.2	9.61
PU-X	−30.0	140.0	7.86
PU-T	−6.7	—	—

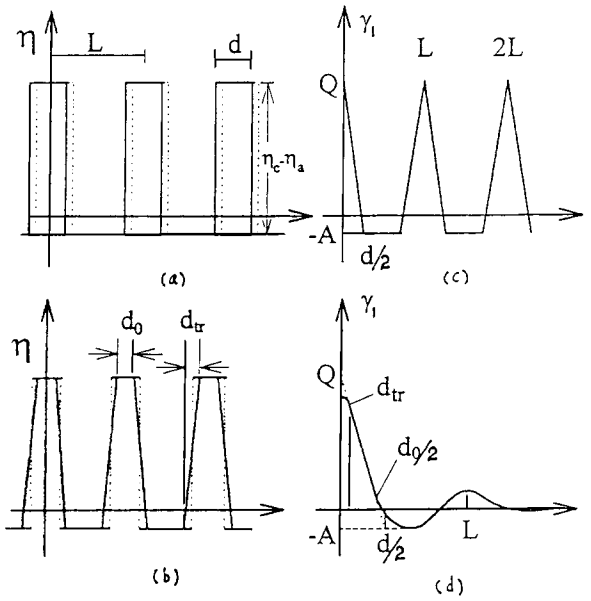

Figure 7 (a) Electron density distribution function $\eta(r)$ of ideal lamellar two phase structure where η_c = electron density of crystalline and η_a = electron density of amorphous region; (b) electron density distribution function $\eta(r)$ of real lamellar two phase structure; (c) 1-D correlation function $\gamma_1(r)$ of ideal lamellar two phase structures; (d) 1-D correlation function $\gamma_1(r)$ of real two phase structure.

functions $\eta(r)$ of ideal [Fig. 7(a)] and real [Fig. 7(b)] lamellar two-phase structures, respectively, while the right hand side are the 1-D correlation functions $\gamma_1(r)$ for the ideal [Figure 7(c)] and real [Fig. 7(d)] lamellar two-phase structures, respectively. In Figure 7, the effect of long-spacing variation, thickness fluctuation, and diffuse boundaries on the shape of electron density distribution function η [Fig. 7(b)] and correlation function γ_1 [Fig. 7(d)] for real lamellar structures are clearly shown. The interdomain spacing (L) was estimated from the first peak position of $\gamma_1(r)$ function and the transition zone (d_{tr}) was estimated from the position near the origin where $\gamma_1(r)$ deviates from the linear region. Figure 8 is the normalized $\gamma_1(r)$ functions for PU-M, PU-X, and PU-T. The L and d_{tr} values estimated from $\gamma_1(r)$ correlation functions for PU-M, PU-X, and PU-T are also listed in Table VI. From Table VI, it is obvious that these three polyurethanes have the following order of L and Q values: PU-M > PU-X > PU-T. However, the order of d_{tr} value for these three polyurethanes are: PU-T > PU-X > PU-M. These results are quite consistent with the DSC results. In the DSC data, T_m and heat of fusion DH for the hard segment of the three polyurethanes are in the following order: PU-M > PU-X > PU-T. The T_g of the soft segment for the three polyurethanes are in the following order: PU-T > PU-X > PU-M. These experimental data revealed that PU-M has the highest degree of hard segment crystallinity, while PU-T has the highest degree of interphase mixing of the hard and soft segments.

Comparing the chemical structures of these three diisocyanates, we may conclude that the results of DSC and SAXS analyses were quite reasonable. In these three diisocyanates, MDI has a chemical structure with a highest degree of symmetry, which leads to the formation of the highest degree of intermolecular hydrogen bond. Thus, PU-M has a highest degree of hard segment crystallinity and also a highest degree of hard- and soft-segment phase separation. Because the diisocyanate on benzene ring are substituted at meta positions to each other, the degree of symmetries of the chemical structures of XDI and TDI are similar but are lower than that of MDI. However, the presence of $-CH_3$ side chain on the benzene ring of TDI seriously steric hindered the formation of hard segment intermolecular hydrogen bond. Thus, PU-T has a lowest degree of hard segment crystallinity and highest degree of soft- and hard-segment phase mixing.

CONCLUSIONS

In the present work, three polyurethanes, i.e., PU-M, PU-X, and PU-T, were synthesized from aliphatic polyester–diol soft segment and butanediol chain extender with three diisocyanates, i.e., MDI, XDI, and TDI, respectively. The DSC and SAXS data revealed that PU-M had the highest degree of hard-segment crystallinity and lowest degree of hard- and soft-segment interphase mixing, while PU-T had the lowest degree of hard segment crys-

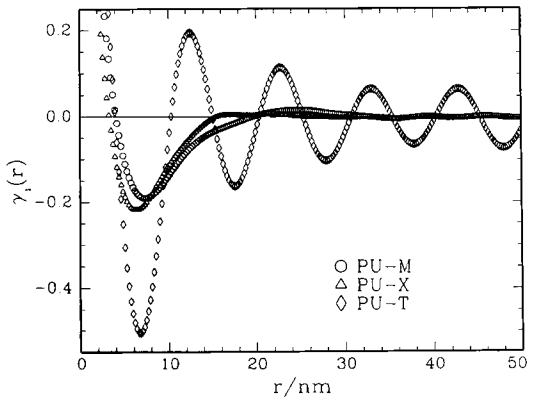

Figure 8 Normalized $\gamma_1(r)$ correlation function of SAXS curves for PU-M, PU-X, and PU-T.

Table VI SAXS Parameters of Polyurethanes

Samples	d_{tr} (nm)	L (nm)		Q (a.u.)
		$\gamma_1(r)$ (Fig. 8)	Bragg [Eq. (10)]	
PU-M	0.89	24.8	16.8	1.00
PU-X	0.90	21.7	14.0	0.975
PU-T	1.95	12.5	5.98	0.0886

tallinity but the highest degree of hard- and soft-segments interphase mixing. The degrees of hard segment crystallinity and interphase mixing of hard and soft segment for PU-X located between PU-M and PU-T. The TGA data for three polyurethanes indicated that PU-X synthesized from alkyl isocyanate and alkyl alcohol had the highest thermal stability. Polyurethanes from aryl isocyanate and alkyl alcohol (PU-M and PU-T) had worse thermal stabilities than PU-X. However, owing to a higher degree of hard segment crystallinity, PU-M had a better thermal stability than PU-T.

This work has been funded by Far Eastern Textile Co. Ltd. under contract number CFF 83005.

REFERENCES

1. Z. S. Petrovic and J. Budinshv-Simendic, *Rubber Chem. Technol.*, **58,** 685 (1985).
2. P. Wright and A. Cumming, in *Solid Polyurethane Elastomers,* Maclaren and Sons, London, 1969.
3. R. Bonart and F. H. Mueller, *J. Macromol. Sci., Phys. Ed.*, **B10,** 177 (1974).
4. S. L. Cooper and A. V. Tobolsky, *J. Appl. Polym. Sci.*, **10,** 1837 (1966).
5. R. Bonart, *Polymer,* **20,** 1389 (1979).
7. Z. S. Petrovic, Z. Zavarge, J. H. Flynn, and W. J. Macknight, *J. Appl. Polym. Sci.*, **51,** 1087 (1994).
8. R. Vieweg and A. Hochtlen, *Kunstoff-Handbuch, Band VII, Polyurethane,* Carl Hanser Verlag, Munchen, 1966, p. 37.
9. P. Debye and A. M. Bueche, *J. Appl. Phys.*, **20,** 5518 (1949).
10. G. Porod, *Kolloid-Z. Z. Polym.*, **124,** 83 (1951).
11. W. Ruland, *J. Appl. Crystallogr.*, **4,** 70 (1971).
12. Z. Petrovic and J. Ferguson, *Hemigska Indust.*, **9,** 618 (1978).
13. J. H. Flynn and L. A. Wall, *Polym. Lett.*, **5,** 192 (1967).
14. J. H. Flynn, in *Thermal Methods in Polymer Analysis,* S. W. Shalaby, Ed., The Franklin Institute Press, Philadelphia, 1978, pp. 163–186.
15. T. Qzawa, *Bull. Chem. Soc. Jpn.*, **38,** 1881 (1965).
16. J. H. Flynn and L. A. Wall, *Polym. Lett.*, **4,** 323 (1966).
17. W. L. Chang, *J. Appl. Polym. Sci.*, **53,** 1759 (1994).
18. F. H. Sanchez and R. V. Graziano, *J. Appl. Polym. Sci.*, **46,** 571 (1992).
19. J. C. M. Torfs, L. Deij, A. J. Dorrepaal, and J. C. Heijens, *Anal. Chem.*, **56,** 2863 (1984).
20. H. E. Kissinger, *Anal. Chem.*, **29,** 1702 (1957).
21. K. C. Frisch, in *Polyurethane Technology,* P. F. Bruins, Ed., Interscience, New York, 1969.
22. M. Kaplan and G. Wooster, *J. Paint Technol.*, **41,** 537 (1969).
23. R. J. Knopf and T. K. Brotherton, *J. Chem. Eng. Data,* **12,** 421 (1967).
24. T. R. Hesketh, J. W. C. van Bogart, and S. L. Cooper, *Polym. Eng. Sci.*, **20,** 19 (1980).
25. L. M. Leung and J. T. Koberstein, *Macromolecules,* **19,** 706 (1986).
26. G. R. Strobl and M. Schneider, *J. Polym. Sci., Polym. Phys.*, **18,** 1343 (1980).
27. L. E. Alexander, *X-Ray Diffraction Methods in Polymer Science,* Wiley-Interscience, New York, 1969.
28. E. W. Fischer, H. Goddar, and G. F. Schmidt, *Makromol. Chem.*, **118,** 144 (1968).
29. B. Crist and N. Morosoff, *J. Polym. Sci., Polym. Phys. Ed.*, **11,** 1023 (1973).

Received January 11, 1996
Accepted May 23, 1996